A Comparative Assessment of Advanced Bias Correction Methods for GPM IMERG in Banjir Kanal Timur Watershed

Rahmah Dara Lufira
Doctoral Program in Water Resources Engineering, Universitas Brawijaya, Malang, Indonesia
rahmahdara@ub.ac.id (corresponding author)

Ery Suhartanto
Department of Water Resources Engineering, Universitas Brawijaya, Malang, Indonesia
erysuhartanto@ub.ac.id

Ussy Andawayanti
Department of Water Resources Engineering, Universitas Brawijaya, Malang, Indonesia
uandawayanti@ub.ac.id

Runi Asmaranto
Department of Water Resources Engineering, Universitas Brawijaya, Malang, Indonesia
runi_asmaranto@ub.ac.id

Rizki Tri Utami
Master's Program in Water Resources Engineering, Universitas Brawijaya, Malang, Indonesia
rizkitriutami16@student.ub.ac.id

Received: 15 October 2025 | Revised: 29 November 2025 | Accepted: 15 December 2025

 DOI: https://doi.org/10.48084/etasr.15484

ABSTRACT

Reliable precipitation inputs are essential for flood risk management in the Semarang lower Banjir Kanal Timur (BKT) watershed, where tidal effects and convective storms play a significant role. This study uses monthly data (2014–2023) from three gauges and GPM IMERG Final Run to evaluate five bias correction methods: Linear Scaling (LS), Linear Regression (LR), Correction Factor (CF), Spatiotemporal (ST), and Random Forest (RF). The analysis follows a reproducible gauge–satellite workflow. Skill was assessed with Nash–Sutcliffe efficiency (*NSE*), Pearson correlation coefficient (*R*), and the ratio of RMSE to standard deviation (RSR). RF yielded the highest performance (*NSE* = 0.61, *R* = 0.78, and *RSR* = 0.63), indicating improved variance reproduction and association. CF and ST attained satisfactory operational skills (both *NSE* = 0.53, *R* = 0.73, and *RSR* = 0.69), while LS and LR yielded modest gains (*NSE* = 0.37 and 0.28; *R* = 0.70 and 0.65; *RSR* = 0.79 and 0.84), reflecting persistent intensity and season-dependent biases and point pixel mismatch. This study provides a decade-long, practice-oriented benchmark for bias correcting IMERG in a tidally influenced tropical urban basin and establishes a consistent monthly performance hierarchy (RF > CF ≈ ST > LS > LR). The resulting bias-corrected series enhances GPM IMERG suitability for hydrological modelling, flood forecasting, and monitoring in data-scarce tropical cities, while highlighting needs for tail-focused evaluation and temporally blocked validation to strengthen operational deployment.

Keywords-GPM IMERG; bias correction; Banjir Kanal Timur watershed; satellite rainfall estimation; hydrological modeling

I. INTRODUCTION

Urban flooding in the Semarang lower watershed, particularly along the Banjir Kanal Timur (BKT), is exacerbated by the concurrence of tidal effects and short-duration convective rainfall. Robust hydrological analysis, therefore, depends on reliable precipitation inputs. However, Indonesian rain-gauge networks are sparse and discontinuous,

and uncorrected satellite estimates often remain biased for operational use in urban basins [1]. At the national scale, TRMM-based analyses partition Indonesia into three dominant rainfall regimes: monsoonal, anti-monsoonal, and semi-monsoonal. These studies also report regime shifts in several regions, providing essential context for rainfall characterization in Semarang [2]. Complementary EO-based investigations have examined long-term spatiotemporal patterns of rainfall intensities in other tropical regions, highlighting the value of satellite and gridded datasets for characterizing variability across scales [3]. The GPM mission's IMERG product offers near-real-time, high-resolution precipitation estimates, yet systematic errors arise from retrieval assumptions, sampling limitations, and point-to-pixel representativeness mismatch issues that are pronounced in convectively active, tidally influenced lowlands such as BKT [4]. Similar performance assessments of global EO-based precipitation products against reference rainfall datasets have reported region- and scale-dependent biases, underscoring the need for careful evaluation and correction before hydrological use [5]. Bias correction is therefore a prerequisite to reconcile IMERG with gauges before hydrological application.

This study provides an operational, decade-long assessment of bias-correction schemes for IMERG in a tropical lower-watershed urban watershed in Indonesia. Using monthly IMERG Final Run and three gauges (2014–2023), by implementing a reproducible gauge satellite workflow with strict quality control, point sampling at gauge locations, Thiessen aggregation, and benchmark five approaches, Linear Scaling (LS), Linear Regression (LR), Correction Factor (CF), Spatiotemporal (ST), and Random Forest (RF). Performance is evaluated with Nash–Sutcliffe efficiency (NSE), Pearson correlation coefficient (R), and the ratio of RMSE to standard deviation (*RSR*). The study hypothesizes that methods capturing nonlinear, season-dependent error structures will outperform LR, while interval-based and ST operational schemes will provide sufficient monthly skill for use in data-scarce tropical urban basins.

II. MATERIALS AND METHODS

A. Study Area and Data Collection

BKT watershed in Semarang is a 55.36 km^2 flood-control system near 6°58' 0" S and 110°25'0" E, built in the Dutch era and central for flood mitigation [6]. A 2014–2023 record of monthly precipitation from three gauges (Maritim, Simongan, and Pucanggading) and the GPM IMERG Final Run V06 was analyzed, yielding 120 monthly pairs. The gauges are maintained by the Indonesian Agency for Meteorology, Climatology, and Geophysics (BMKG) and local water resources agencies. GPM IMERG Final Run is available at approximately 0.1° (~10 km) spatial resolution and sub-daily temporal frequency; over the relatively small 55.36 km² BKT watershed. This effectively corresponds to a single IMERG grid cell within which all three gauges are located or lie immediately adjacent. The native sub-daily IMERG estimates were aggregated to monthly totals to match the gauge record and to support a decade-long bias-correction benchmark over 2014–2023.

Preprocessing applied a double-mass curve, Thiessen watershed averages, point sampling of IMERG at gauge sites, and temporal alignment. Inputs were screened using *NSE* and *R* [7]. Because the available IMERG gauge overlap spans only 10 hydrological years (2014–2023), the full set of 120 monthly gauge-satellite pairs was used for both model fitting and performance assessment, without a separate calibration validation split; the reported skill metrics therefore describe in-sample agreement over the benchmark period rather than independent out-of-sample validation. Monthly aggregation improves robustness to noise and gaps, addresses point grid, and sub-pixel heterogeneity [8]. Figure 1 shows the study area at the BKT watershed.

B. LS Method

LS applies a constant multiplicative factor to align the climatological mean of satellite estimates with that of gauge observations. For each station, the Scaling Factor (SF) is defined as the ratio of the mean observed monthly precipitation ($\bar{P}_{obs}$) to the mean satellite monthly precipitation ($\bar{P}_{sat}$) over the analysis period:

$$SF = \frac{\bar{P}_{obs}}{\bar{P}_{sat}},\ P^*_{sat,t} = SF \times P_{sat,t} \quad (1)$$

where overbars denote monthly means computed from the 2014–2023 record, and t indexes the month. Applying the derived SF to the original IMERG series yields a bias-corrected product that is more consistent with gauge observations and subsequent hydrological analyses [9].

C. LR Method

A station-wise simple LR was used to adjust satellite estimates using gauge observations, with the monthly precipitation modeled as:

$$P_{obs,t} = a + b\,P_{sat,t} + \varepsilon t \quad (2)$$

where $P_{obs,t}$ and $P_{sat,t}$ denote observed (gauge) and satellite-derived precipitation in mm/month at month *t*; and *a* and *b* are the intercept and slope; and *εt* is the residual error. Coefficients *a* and *b* were estimated by ordinary least squares from the full 2014–2023 monthly record, and the bias-corrected series was obtained as:

$$P_{corrected} = a + b\,P_{sat,t} \quad (3)$$

Model adequacy was evaluated using residual diagnostics, including assessments of linearity and homoscedasticity. Consistent with the study protocol, agreement between corrected and observed series over 2014–2023 was quantified using the *NSE*, *R*, and *RSR* [10].

D. CF Method

This study adopts the CF approach recommended by Indonesia's Ministry of Public Works and Public Housing (PWPH). The CF was derived through a piecewise stratification of rainfall intervals, adapted from empirical hydrological engineering standards, and through an iterative error minimization procedure [11]. The formulation is expressed as:

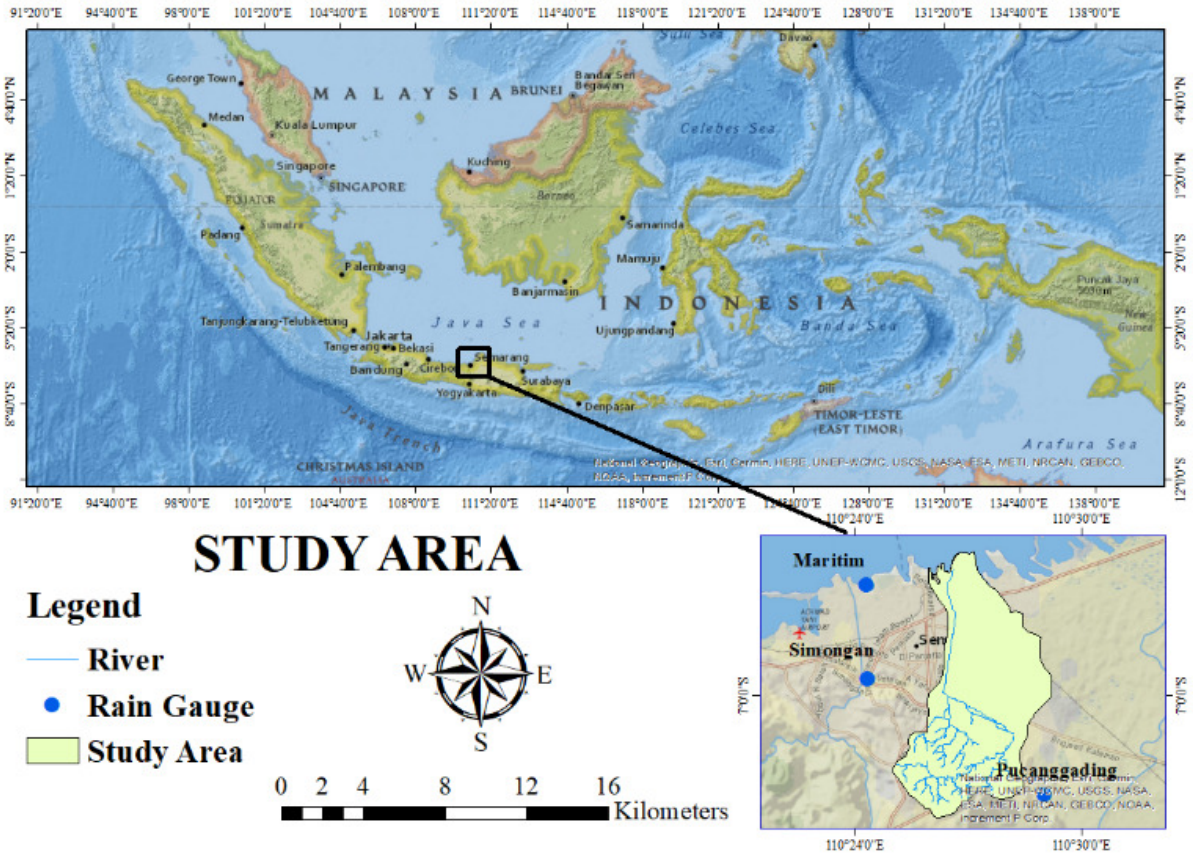

Fig. 1. Study area at the BKT watershed.

$$P_{corrected} = C_i \times P_{GPM} \text{ for } P_{GPM} \in [I_i, I_{i+1}] \quad (4)$$

where $P_{corrected}$ is the corrected satellite precipitation, P_{GPM} is the original GPM estimate, and C_i is the correction coefficient for the rainfall interval $[I_i, I_{i+1}]$. Once calculated, this CF is applied to the satellite precipitation dataset by multiplying it with the original satellite estimates. This adjustment aims to align the satellite-derived measurements with ground-based observations more closely, thereby improving the data's reliability for various applications [12].

E. ST Method

Satellite data are inherently subject to Spatio-temporal variability due to factors such as topography and atmospheric conditions, making this analysis vital for improving the accuracy of precipitation estimates. Temporal analysis is conducted across different time scales by aggregating precipitation data into daily, monthly, seasonal, or annual intervals, allowing researchers to observe how precipitation trends and patterns evolve. Techniques such as time series analysis can be applied to detect seasonality, trends, and anomalies in the data, enabling an examination of routine and extreme weather events [13]. Temporal analyses also facilitate the comparison of satellite estimates against historical data to assess improvements over time or shifts in precipitation regimes due to climate variability [14]. In the present study, monthly spatio-temporal correction was implemented by applying grid-wise temporal adjustment factors based on local gauge–satellite discrepancies.

F. RF Method

RF regression was applied to correct biases in GPM IMERG monthly rainfall by learning a nonlinear mapping from satellite estimates to gauge observations. The RF is trained on temporally matched gauge IMERG monthly pairs (2014–2023) using predictors comprising raw IMERG precipitation, site coordinates, elevation, month of year encoded with sine cosine harmonics, and simple neighborhood statistics to capture spatial and seasonal dependencies. RF hyperparameters (e.g., number of trees, maximum depth, minimum samples per leaf) were selected via grid search on the full 2014–2023 record using *NSE* and *R* as performance criteria. RF is utilized because it models nonlinear links between satellite rainfall and topography climate while accommodating spatial dependence. Spatial RF frameworks often outperform traditional regression and yield variable-importance diagnostics that support interpretability in operational settings [15]. Post-training, RF predictions replace IMERG values monthly, producing a gauge-consistent, bias-corrected product evaluated using *NSE*, *R*, and *RSR*. Consistent with the data, all 120 monthly gauge–satellite pairs were used for both model fitting and performance assessment, so the reported RF skill represents in-sample performance over the 2014–2023 benchmark period rather than independent out-of-sample validation.

III. RESULTS AND DISCUSSION

A. LS Method

LS improved the agreement between IMERG and gauges, with *NSE* = 0.37, R = 0.70, and RSR = 0.79, indicating a moderate gain in mean alignment but limited skill in reproducing month-to-month variability and extremes. This result reflects the limitation of using a single multiplicative factor based on 2014–2023 averages. The method cannot capture seasonal or intensity-dependent biases, and the mismatch between satellite pixels and point gauges adds additional error. Increased temporal aggregation is known to enhance gauge satellite correspondence, aligning with the monthly results [16]. As a transparent baseline, LS preserves temporal ordering yet fails to correct distributional discrepancies; in contrast, distribution-aware or hybrid approaches can better address these inconsistencies when paired with robust preprocessing. Figure 2 shows a consistent but dispersed scatter (*NSE* = 0.37, *R* = 0.70, and *RSR* = 0.79) and time-series patterns of peak underestimation and minor-event overestimation, underscoring LS's constraints in convectively complex settings while confirming its practicality in data-limited contexts.

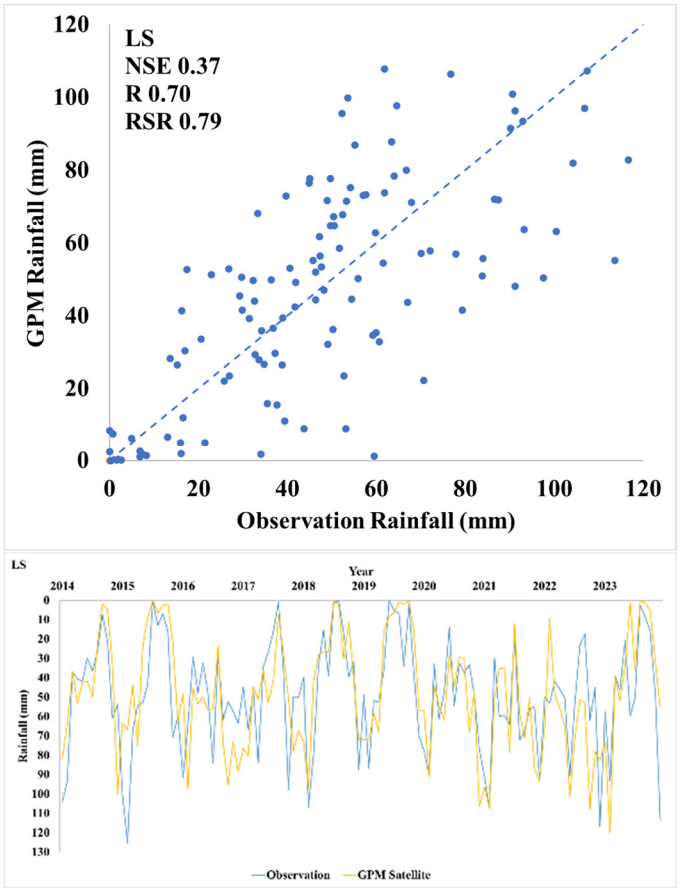

Fig. 2. Comparison of GPM satellite rainfall and observed rainfall using the LS method.

B. LR Method

The LR method yielded an *NSE* of 0.28, an *R* value of 0.65, and an *RSR* of 0.84, indicating limited skill in reproducing monthly variability. Station-wise ordinary least squares were fit to the full 2014–2023 record, using observed rainfall as the response and IMERG monthly totals as the predictor. Although the positive slope shows that larger satellite estimates generally track higher observations, pronounced dispersion, especially at higher totals, reveals weak predictive capacity under nonlinear, heteroscedastic error structures typical of intensity and season-dependent biases [17]. Consistently, Figure 3 exhibits wide scatter and time series patterns of peak underestimation with low intensity overestimation; residual diagnostics corroborate these effects.

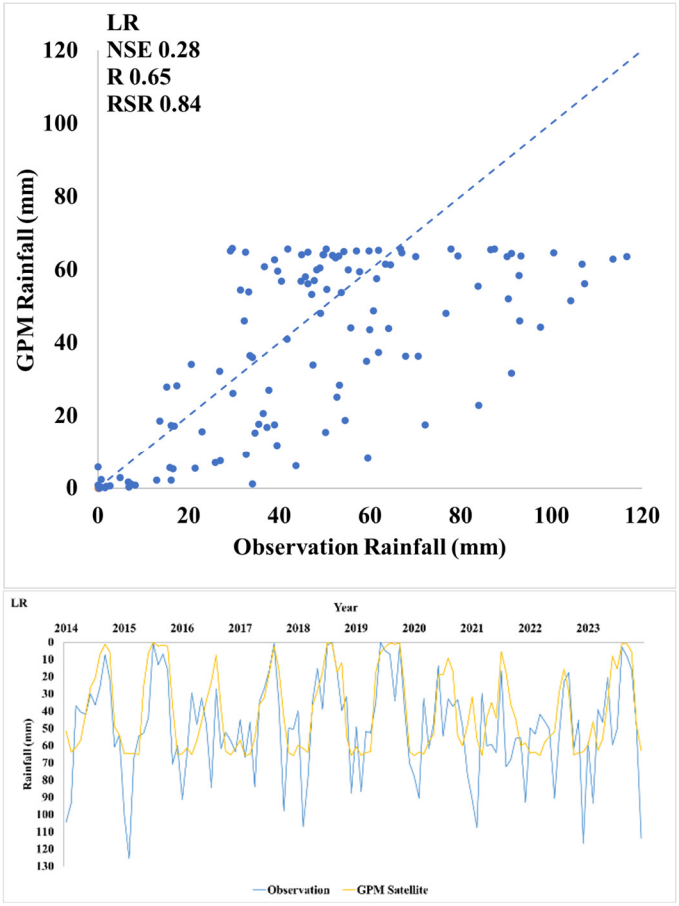

Fig. 3. Comparison of GPM satellite rainfall and observed rainfall using the LR method.

C. CF Method

The CF method achieved an *NSE* of 0.53, R value of 0.73, and RSR of 0.69, indicating satisfactory monthly skill coherent temporal variability with remaining magnitude discrepancies consistent with hydrological interpretive thresholds. In this study, monthly IMERG totals were stratified into rainfall intervals, and interval-specific multiplicative coefficients were applied; this piecewise design directly targets intensity-dependent errors that global rescaling cannot address. Figure 4 reflects these mechanics: the scatter shows tighter clustering

than LS and LR, and the time series aligns more closely during moderately high months, with residual peaks expected from bin-constant coefficients. Calibrated factors decrease monotonically with intensity (0.89 for 0–50 mm; 0.52 for 50–100 mm; 0.25 for 100–300 mm; 0.16 for 300–500 mm; and 0.10 for >500 mm), consistent with IMERG wet-month overestimation. Operationally, CF is transparent, easy to update, and reproducible in data-scarce settings, though it does not surpass the best-performing method (RF) in experiments; rather, it offers a strong, communicable baseline that balances skill and simplicity [18].

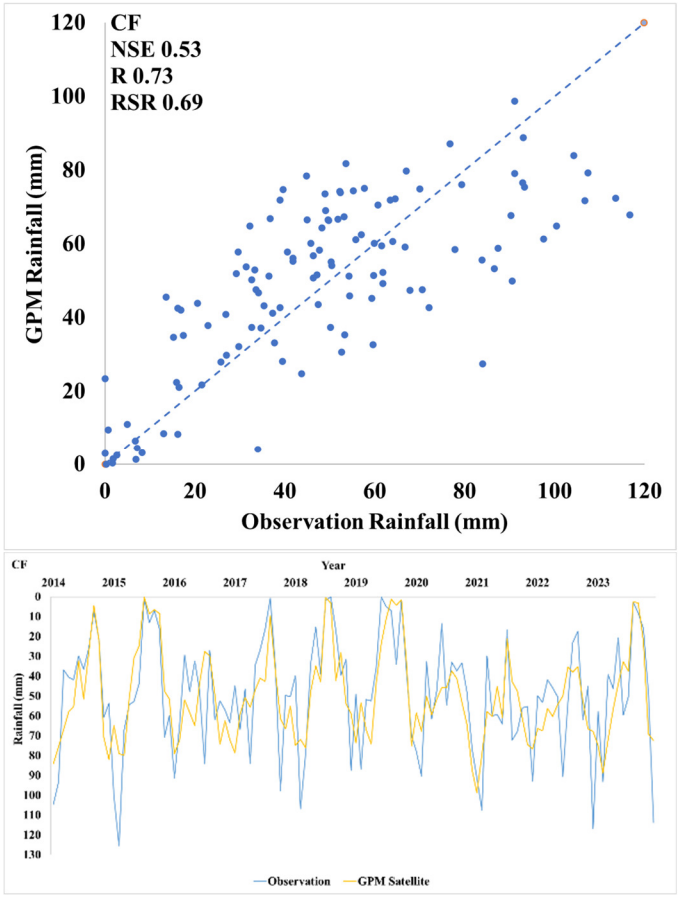

Fig. 4. Comparison of GPM satellite rainfall and observed rainfall using the CF method.

D. ST Method

The ST method achieved NSE = 0.53; R = 0.73; and RSR = 0.69, indicating moderate skill: temporal trends and seasonal variability are reasonably captured, while intensities at low and extreme events remain difficult to quantify patterns consistent with the influence of spatial heterogeneity and temporal dynamics on satellite-precipitation accuracy [19]. Enhancements typically involve higher spatio-temporal resolution, terrain-specific adjustments, and satellite gauge fusion; adopting ST models can better represent nonlinear rainfall dynamics and improve operational forecasting performance [20].

Although daily IMERG and gauge data were available, monthly aggregation was used to reduce noise and gaps, aiding trend comparison but attenuating short-duration, high-intensity events and contributing to residual errors at extremes. Consistently, Figure 5 shows tighter scatter than simpler methods and improved temporal alignment in mid-range rainfall, with discrepancies at peaks and lows. Subregion analysis over lowlands yielded stable performance.

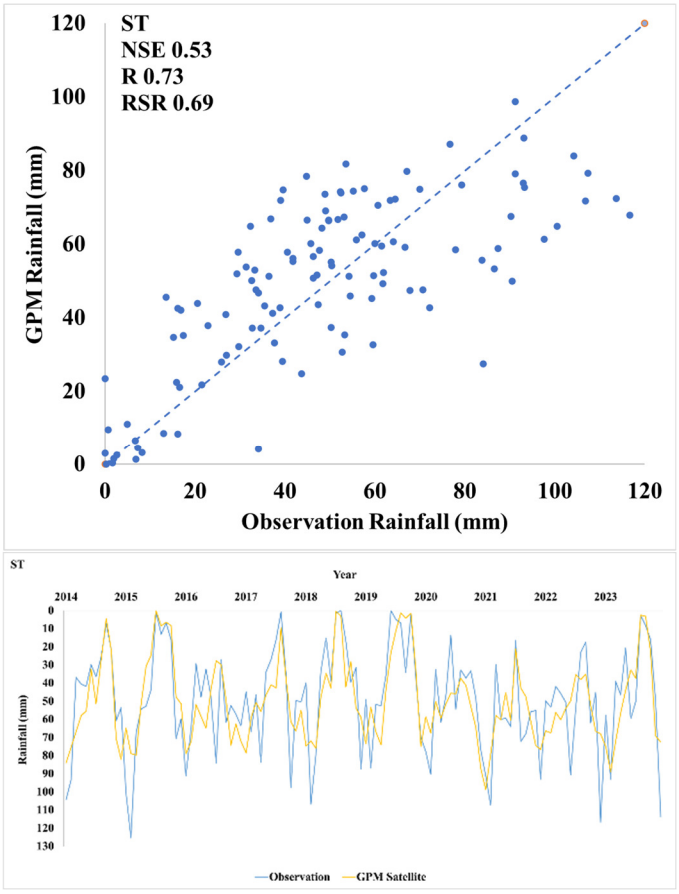

Fig. 5. Comparison of GPM satellite rainfall and observed rainfall using the ST method.

E. RF Method

RF bias correction achieved the best performance among all tested methods, with an *NSE* of 0.61, R value of 0.78, and *RSR* of 0.63, over the 2014–2023 monthly record, as seen in Figure 6. In the present study, RF was used strictly as a bias-correction mapping from IMERG monthly totals and simple topo-seasonal descriptors to gauge totals. Points clustered near the 1:1 line indicate effective removal of systematic bias; a slight widening of scatter at the highest totals suggests residual underestimation during the wettest months, patterns also reported for IMERG [25] post-processing elsewhere. Methodologically, ensemble trees are robust to multicollinearity and skewed errors, and their variable-importance diagnostics support interpretability in operational settings. RF's ability to model nonlinear intensity season interactions explains its superior association and variance reproduction relative to LS/LR/CF/ST.

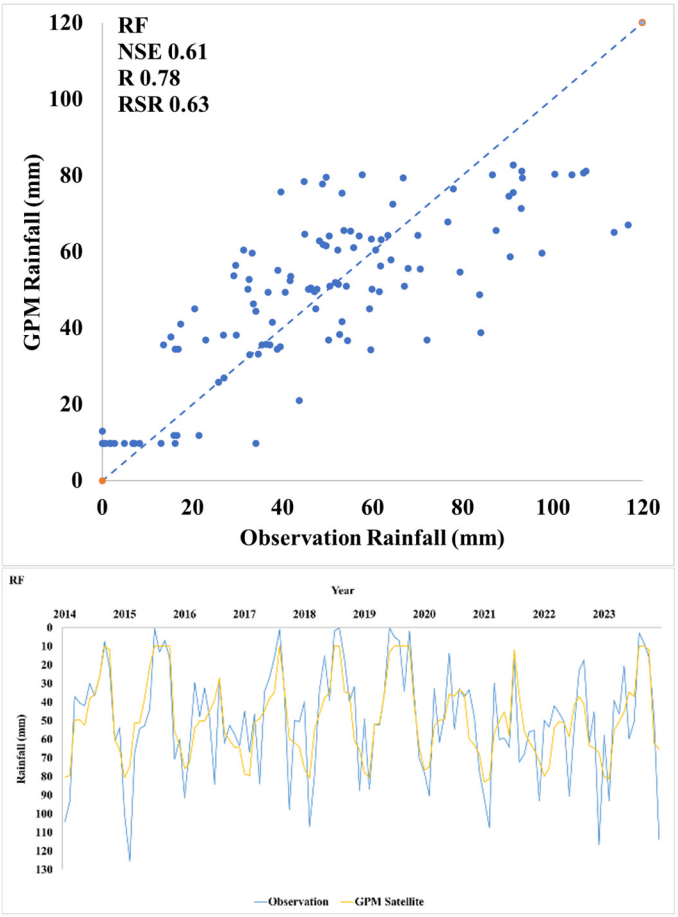

Fig. 6. Comparison of GPM satellite rainfall and observed rainfall using the RF method.

RF is a competitive and economical option for near-real-time applications in tropical urban basins, with scope for tail-focused refinements to better capture extremes [21]. These performance metrics represent in-sample agreement over the 2014–2023 benchmark period, consistent with the use of the full record for model fitting described in the Materials and Methods section. Despite satisfactory performance, the study is limited by the small number of gauges, the mismatch between the ~10 km IMERG grid and point-scale observations, and the use of monthly aggregation of an inherently sub-daily product, which together may reduce sensitivity to short-duration, highly localized convective extremes. Future work should therefore consider higher temporal resolutions, denser or complementary validation datasets, and more explicit treatment of point–pixel representativeness errors.

As presented in Table I, RF is the top-performing method, with an *NSE* of 0.61, *R* value of 0.78, and *RSR* of 0.63, exceeding commonly used interpretive thresholds for monthly hydrological applications and indicating a good reproduction of both temporal association and variance. CF and ST form a second tier of performance with identical skill (*NSE* = 0.53, *R* = 0.73, and *RSR* = 0.69), providing consistent temporal co-variation but retaining a magnitude bias that reflects remaining intensity-dependent errors. In contrast, LS and LR increase correlation (*R* = 0.70 and 0.65, respectively) but yield unsatisfactory efficiency (*NSE* = 0.37 and 0.28, and *RSR* = 0.79 and 0.84), highlighting that a single multiplicative factor or a global linear mapping cannot adequately correct season- and intensity-dependent biases in convectively active urban basins [22].

CF and ST outperform LS/LR because they explicitly target the error structure: interval-based coefficients counter wet-month overestimation, and limited site-specific adjustments help stabilise recurring departures [23]. RF attains the highest skill by learning nonlinear relations between IMERG totals and simple topo-seasonal descriptors, consistent with evidence that RF-based post-processing can surpass classical regression and interpolation-only schemes [24]. Although residual spread in the wettest months still points to the need for tail-focused refinements. Taken together, these results establish a clear performance hierarchy RF > CF ≈ ST > LS > LR, which is consistent with known challenges of satellite-gauge reconciliation in heterogeneous lowland basins and with the reported capabilities and limitations of the respective methods in the literature.

TABLE I. ACCURACY COMPARISON OF BIAS CORRECTION METHODS (VALIDATION PERIOD: 2014–2023)

Method	*NSE*	*R*	*RSR*
LS	0.37	0.70	0.79
LR	0.28	0.65	0.84
CF	0.53	0.73	0.69
ST	0.53	0.73	0.69
RF	0.61	0.78	0.63

IV. CONCLUSION

This study provides a decade-long operational benchmark of five bias correction methods for GPM IMERG monthly precipitation in the tidally influenced lower Banjir Kanal Timur (BKT) urban basin. Using a reproducible gauge satellite workflow, strict quality control, point sampling at gauges, and Thiessen aggregation, the study establishes a consistent monthly performance hierarchy: Random Forest (RF)>Correction Factor (CF) ≈ Spatiotemporal (ST) >Linear Scaling (LS)>Linear Regression (LR). RF attains the highest skill with Nash–Sutcliffe efficiency (*NSE*) of 0.61, Pearson correlation coefficient (*R*) value of 0.78, and the ratio of RMSE to standard deviation (*RSR*) of 0.63. The CF and ST achieve satisfactory performance, with an *NSE* of 0.53, *R* value of 0.73, and *RSR* of 0.69, and serve as transparent, operational baselines. LS and LR yield limited gains, with *NSE* = 0.37 and 0.28; *R* = 0.70 and 0.65; and *RSR* = 0.79 and 0.84, reflecting reduced capacity to address intensity-dependent and seasonal biases. This study provides a practical and reproducible benchmark for tropical, tidally influenced urban watersheds. It combines engineering-based corrections with interpretable machine-learning methods to produce bias-corrected rainfall series useful for flood forecasting and hydrological modeling. The study has some limitations, including hyperparameter selection on the full record and reliance on monthly aggregation, which may mute short-duration extremes. Future studies should extend the proposed methods to daily or hourly

IMERG datasets and apply cross-regional testing to verify generalizability.

ACKNOWLEDGEMENT

The authors thank data providers, including the Water Resources Public Works Agency (WRPWA) of Central Java and the River Basin Authority (RBA) Pemali Juana. The authors also express their appreciation to all the parties and stakeholders for their assistance in this study.

REFERENCES

[1] M. Tan and Z. Duan, "Assessment of GPM and TRMM Precipitation Products over Singapore," *Remote Sensing*, vol. 9, no. 7, July 2017, Art. no. 720, https://doi.org/10.3390/rs9070720.

[2] H. Kuswanto, D. Setiawan, and A. Sopaheluwakan, "Clustering of Precipitation Pattern in Indonesia Using TRMM Satellite Data," *Engineering, Technology & Applied Science Research*, vol. 9, no. 4, pp. 4484–4489, Aug. 2019, https://doi.org/10.48084/etasr.2950.

[3] N. Awasthi *et al.*, "Long-Term Spatiotemporal Investigation of Various Rainfall Intensities over Central India Using EO Datasets," *Hydrology*, vol. 11, no. 2, Feb. 2024, Art. no. 27, https://doi.org/10.3390/hydrology11020027.

[4] Y. Derin *et al.*, "Evaluation of GPM-Era Global Satellite Precipitation Products over Multiple Complex Terrain Regions," *Remote Sensing*, vol. 11, no. 24, Dec. 2019, Art. no. 2936, https://doi.org/10.3390/rs11242936.

[5] N. Awasthi, J. N. Tripathi, G. P. Petropoulos, D. K. Gupta, A. K. Singh, and A. K. Kathwas, "Performance Assessment of Global-EO-Based Precipitation Products against Gridded Rainfall from the Indian Meteorological Department," *Remote Sensing*, vol. 15, no. 13, July 2023, Art. no. 3443, https://doi.org/10.3390/rs15133443.

[6] S. Suripin and D. Kurniani, "Pengaruh Perubahan Iklim terhadap Hidrograf Banjir di Kanal Banjir Timur Kota Semarang," *Media Komunikasi Teknik Sipil*, vol. 22, no. 2, Dec. 2016, Art. no. 119, https://doi.org/10.14710/mkts.v22i2.12881.

[7] D. Zhang, X. Liu, P. Bai, and X.-H. Li, "Suitability of Satellite-Based Precipitation Products for Water Balance Simulations Using Multiple Observations in a Humid Catchment," *Remote Sensing*, vol. 11, no. 2, Jan. 2019, Art. no. 151, https://doi.org/10.3390/rs11020151.

[8] A. Lombardi *et al.*, "On the Combined Use of Rain Gauges and GPM IMERG Satellite Rainfall Products for Hydrological Modelling: Impact Assessment of the Cellular-Automata-Based Methodology in the Tanaro River Basin in Italy," *Hydrology and Earth System Sciences*, vol. 28, no. 16, pp. 3777–3797, Aug. 2024, https://doi.org/10.5194/hess-28-3777-2024.

[9] A. H. Azman, N. N. A. Tukimat, and M. A. Malek, "Analysis of Linear Scaling Method in Downscaling Precipitation and Temperature," *Water Resources Management*, vol. 36, no. 1, pp. 171–179, Jan. 2022, https://doi.org/10.1007/s11269-021-03020-0.

[10] A. Akbas and H. Ozdemir, "Comparing Satellite, Reanalysis, Fused and Gridded (In Situ) Precipitation Products Over Türkiye," *International Journal of Climatology*, vol. 44, no. 16, pp. 5873–5889, Dec. 2024, https://doi.org/10.1002/joc.8671.

[11] *Analisis Curah Hujan*. Jakarta, Indonesia: Ministry of Public Works and Public Housing, 2022.

[12] R. Andari, N. Nurhamidah, D. Daoed, and Marzuki, "Evaluation of Bias Correction Methods for Multi-Satellite Rainfall Estimation Products," *IOP Conference Series: Earth and Environmental Science*, vol. 1317, no. 1, Mar. 2024, Art. no. 012008, https://doi.org/10.1088/1755-1315/1317/1/012008.

[13] L. Wei, S. Jiang, L. Ren, F. Yuan, and L. Zhang, "Performance of Two Long-Term Satellite-Based and GPCC 8.0 Precipitation Products for Drought Monitoring over the Yellow River Basin in China," *Sustainability*, vol. 11, no. 18, Sept. 2019, Art. no. 4969, https://doi.org/10.3390/su11184969.

[14] A. Huang *et al.*, "Evaluation of Multisatellite Precipitation Products by Use of Ground-based Data Over China," *Journal of Geophysical Research: Atmospheres*, vol. 121, no. 18, Sept. 2016, https://doi.org/10.1002/2016JD025456.

[15] C. Chen, B. Hu, and Y. Li, "Easy-to-Use Spatial Random-Forest-Based Downscaling-Calibration Method for Producing Precipitation Data with High Resolution and High Accuracy," *Hydrology and Earth System Sciences*, vol. 25, no. 11, pp. 5667–5682, Nov. 2021, https://doi.org/10.5194/hess-25-5667-2021.

[16] A. Ochoa, L. Pineda, P. Crespo, and P. Willems, "Evaluation of TRMM 3B42 Precipitation Estimates and WRF Retrospective Precipitation Simulation Over the Pacific–Andean Region of Ecuador and Peru," *Hydrology and Earth System Sciences*, vol. 18, no. 8, pp. 3179–3193, Aug. 2014, https://doi.org/10.5194/hess-18-3179-2014.

[17] I. E. Gbode *et al.*, "Verification of Multiresolution Model Forecasts of Heavy Rainfall Events From 23 to 26 August 2017 Over Nigeria," *Meteorological Applications*, vol. 30, no. 4, July 2023, Art. no. e2135, https://doi.org/10.1002/met.2135.

[18] R. K. Makumbura, J. Manatunge, and U. Rathnayake, "Bridging Data-Driven and Process-Based Approaches for Hydrological Modeling in the Tropics: Insights from the Kelani River Basin, Sri Lanka," *Results in Engineering*, vol. 27, Sept. 2025, Art. no. 105975, https://doi.org/10.1016/j.rineng.2025.105975.

[19] X. Li, L. Wang, H. Zhou, Y. Wang, K. Niu, and L. Li, "The Compound Effect of Spatial and Temporal Resolutions on the Accuracy of Urban Flood Simulation," *Computational Intelligence and Neuroscience*, vol. 2022, pp. 1–12, June 2022, https://doi.org/10.1155/2022/3436634.

[20] Anita Yuliana, Joko Sujono, and Karlina, "Analysis of Extreme Rainfall in the Mt. Merapi Area," *Journal of the Civil Engineering Forum*, pp. 73–84, Dec. 2023, https://doi.org/10.22146/jcef.10084.

[21] X. Yang *et al.*, "Correcting the Bias of Daily Satellite Precipitation Estimates in Tropical Regions Using Deep Neural Network," *Journal of Hydrology*, vol. 608, May 2022, Art. no. 127656, https://doi.org/10.1016/j.jhydrol.2022.127656.

[22] M. Kimani, J. Hoedjes, and Z. Su, "An Assessment of Satellite-Derived Rainfall Products Relative to Ground Observations over East Africa," *Remote Sensing*, vol. 9, no. 5, May 2017, Art. no. 430, https://doi.org/10.3390/rs9050430.

[23] R. Andari, Nurhamidah, D. Daoed, and Marzuki, "Validation of TRMM and GPM Satellite Data Using Daily Precipitation Observations," *International Journal on Advanced Science, Engineering and Information Technology*, vol. 14, no. 2, pp. 555–562, Apr. 2024, https://doi.org/10.18517/ijaseit.14.2.18980.

[24] C. Zhang *et al.*, "Evaluation and Intercomparison of High-Resolution Satellite Precipitation Estimates—GPM, TRMM, and CMORPH in the Tianshan Mountain Area," *Remote Sensing*, vol. 10, no. 10, Sept. 2018, Art. no. 1543, https://doi.org/10.3390/rs10101543.

[25] "Integrated Multi-satellitE Retrievals for GPM (IMERG)," *NASA Global Precipitation Measurement (GPM) Mission*, Dec. 2025. https://gpm.nasa.gov/data/imerg